

Composite Method for the Mixing of Two Steady Laminar Flows

Anthony Demetriades*

Montana State University, Bozeman, Montana 59715

An analytic solution is presented for the steady, two-dimensional mixing of two parallel, laminar, and initially dissimilar streams beyond the trailing edge of a thin partition. The method consists of combining known analytic solutions for flat-plate wakes with Chapman's classic solution for the free shear layer. The key assumptions made are that the wake "component" grows independently of this shear layer component and that the minimum-velocity locus of the former coincides with the zero streamline of the Chapman flow. The initial boundary-layer profiles at the trailing edge are taken to be exponentials with a stretching factor, whose advance choice simulates some common laminar boundary layers. All flow properties are then found in terms of the space coordinates and seven parameters, including this stretching factor, the fast-side Mach number, specific heat ratio, partition temperature, and the ratios of total temperatures, initial stream velocities, and initial momentum thicknesses at the trailing edge. The solutions are closed form, analytic, free of discontinuities, and capable of simulating symmetric or asymmetric wakes, base flows, and the mixing of parallel streams. These results compare closely with well-known numerical results obtained for wakes and base flows.

Nomenclature

a, a'	= independent variables in wake solution [Eqs. (14) and (27)]
b, b'	= independent variables in wake solution [Eqs. (14) and (27)]
B	= constant in wake temperature solution [Eq. (16)]
c, c'	= independent variables in wake solution [Eqs. (15) and (28)]
C	= constant in wake solution [Eq. (16)]
C_n	= polynomial coefficients in free shear layer curve fit [Eqs. (6) and (7)]
d, d'	= independent variables in wake solution [Eqs. (15) and (28)]
\bar{h}	= nondimensional temperature [Eq. (12)]
\bar{h}_0	= initial nondimensional temperature at $x^* = 0$
M	= Mach number
p	= pressure
P	= θ_1/θ_2
P'	= $\theta_1\rho_1/\theta_2\rho_2$
R	= gas constant
Re'	= unit Reynolds number
S	= stretching factor
T	= local temperature
T_0	= stagnation temperature
T_w	= partition temperature
u	= longitudinal velocity
\bar{u}	= nondimensional velocity [Eq. (11)]
\bar{u}_0	= initial nondimensional velocity at $x^* = 0$
x^*	= physical distance beyond trailing edge (Fig. 1)
x'	= nondimensional distance beyond trailing edge [Eq. (2)]
\bar{x}	= nondimensional distance beyond trailing edge [Eq. (17)]
y	= nondimensional lateral distance, $= y^*/\theta_1$
y^*	= physical lateral distance (Fig. 1)
\bar{y}^*	= compressible-transformed lateral distance [Eq. (2)]
y'	= nondimensional lateral distance [Eq. (2)]

y'_m	= location of minimum wake velocity along y'
y''	= nondimensional lateral distance [Eq. (18)]
γ	= specific heat ratio
η	= nondimensional variable in free shear layer analysis [Eq. (4)]
θ	= momentum thickness
ρ	= local density

Subscripts

1	= stream 1 (a constant)
2	= stream 2 (a constant)
e	= constant quantity external to the wake
FSL	= obtained from the free shear layer solution alone

I. Introduction

THE problem addressed in this paper is the mixing of two steady, laminar, two-dimensional streams downstream of the trailing edge of a thin partition. Each stream is uniform outside the boundary layer growing on its side of the partition, as shown in Fig. 1, and its properties (velocity, density, etc.) are known and subscripted by "1" or "2" for the top and bottom streams, respectively. The momentum thicknesses θ_1 and θ_2 at the trailing edge (TE) are also given. The objective of the paper is to solve for the flow properties u, ρ, T , etc., in the region $0 < x^* < \infty, -\infty < y^* < \infty$, where the physical coordinates x^*, y^* are illustrated in Fig. 1.

The two fluids are assumed to be nonreacting, identical, and subject to the perfect gas state equation $p = \rho RT$. In this calculation we will also consider the flow to be isobaric, of unity Prandtl number and constant Chapman-Rubens factor. On the other hand, we shall impose no restrictions on the ratios $(\cdot)_2/(\cdot)_1$, e.g., on $u_2/u_1, T_2/T_1, \theta_2/\theta_1$, etc., or on the θ_2/θ_1 ratio or the flow Mach and Reynolds numbers. Furthermore, we shall allow the given partition temperature T_w to differ from T_{01} by any desired amount. The complete latitude allowed for these input parameters makes it clear that a solution to the general problem of Fig. 1 would also solve for the flow in some specific configurations of considerable interest. For example, $(\cdot)_1 = (\cdot)_2$ would give us the solution for the wake of a thin plate, and $u_2/u_1 = 0$ that of a flow next to a stagnant region (e.g., base or separated flows). The general case $(\cdot)_1 \neq (\cdot)_2 \neq 0$ represents the mixing of two finite parallel streams, of interest to combustion, film cooling, etc.

Solutions to the problem of Fig. 1 are known only for certain special choices of the parameters $(\cdot)_1$ and $(\cdot)_2$. For the incompressible symmetric wake of an adiabatic plate ($M_1 = 0, u_1 = u_2, \theta_1 = \theta_2, T_w = T_0$), solutions were provided long ago by Goldstein¹ for small x^* and asymptotically ($x^* \rightarrow \infty$) by Goldstein² and Tollmien.³ Chapman⁴ provided solutions for the so-called free shear layer adjacent to a stagnant region without initial boundary layers ($u_2 = 0, \theta_1 = \theta_2 = 0$). Applications of Chapman's solution came under intense scrutiny in the 1960s, with numerical solutions⁵ and momentum integral methods⁶ extending these findings to the recirculating flow in the base of an object. In fact, numerical solutions are now quite feasible⁷ for solving the steady, two-dimensional problem of Fig. 1. Details on these developments can be found in Berger.⁸

The present work takes a different approach, aiming at a completely analytic solution of the general problem, in a way allowing special cases (e.g., wakes) to be directly calculated by a choice of the input parameters. This result is achieved by combining two known analytic solutions: one dealing with viscous flow and the other with the inviscid, external flow. Velocity and temperature formulas are obtained that are continuous and valid over the entire x^*, y^* range for any set of chosen conditions $M_1, u_2/u_1, T_{02}/T_{01}$, etc.

II. Outline of the Method

The presence of boundary layers on the partition and the resulting condition $u(x^* = y^* = 0) = 0$ means that the flow will have a "wakelike" character for some distance beyond the TE, whether symmetric or asymmetric, depending on whether $\theta_1 = \theta_2$ or $\theta_1 \neq \theta_2$. This wakelike behavior will diffuse with x^* , but any inviscid asymmetry $(\cdot)_1 \neq (\cdot)_2$ (e.g., $u_1 \neq u_2$) will eventually dominate the flow far downstream. We can therefore think of two "components," a wake component and a free shear layer component, which combine in some manner to configure the total flow. The present method postulates that each component develops independently of the other along x^* and seeks a way to combine them. To maintain analyticity throughout and to fit the solution to requirements at the region boundaries $x^* = 0, \infty$, and $y^* = \pm \infty$, the TE boundary-layer profiles and the free shear layer profile at $x^* = \infty$ will be specified algebraically. For the latter Chapman's solutions⁴ will be used. For the initial boundary-layer velocity profiles we will use an exponential with a stretching factor chosen in advance, which simplifies the algebra and allows some flexibility in simulating laminar viscous flows.

III. Free Shear Layer Component

In the general case we assume that the wakelike flow caused by the partition boundary layers is embedded on an inviscid background generated by the jump condition $(\cdot)_1 \neq (\cdot)_2$. This background flow is the free shear layer (FSL) solved by Chapman⁴ for $u_2 = 0$:

$$\left(\frac{u}{u_1}\right)_{\text{FSL}} = f\left(\tilde{y}^* \sqrt{\frac{Re_1'}{x^*}}\right) = f\left(\frac{y'}{\sqrt{x^*}}\right) \quad (1)$$

where

$$\tilde{y}^* \equiv \int_0^{y^*} \frac{\rho}{\rho_1} dy^*, \quad y' \equiv \frac{\tilde{y}^*}{\theta_1 + \theta_2}, \quad x' \equiv \frac{x^*}{(\theta_1 + \theta_2)^2 Re_1'} \quad (2)$$

For the present purposes this solution must be adjusted to give $f(\tilde{y}^* = \infty) = 1$ and $f(\tilde{y}^* = -\infty) = u_2/u_1$ and, in keeping with the desire to express it analytically, can replace f by a polynomial. Furthermore, we must allow for a lateral displacement of the Chapman profile so that its "zero streamline" can be positioned consistently with the corresponding streamline of the wake component; the rationale for this positioning will be presented further later in the paper.

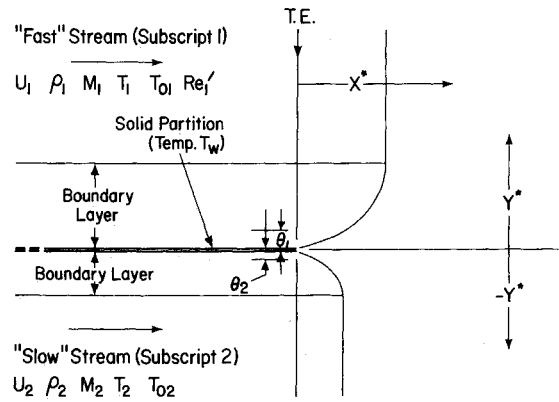


Fig. 1 Flow geometry and nomenclature.

With these modifications the free shear layer solution becomes

$$\left(\frac{u}{u_1}\right)_{\text{FSL}} = \left(1 - \frac{u_2}{u_1}\right) \sum_0^6 C_n \eta^n + \frac{u_2}{u_1} \quad (3)$$

where

$$\eta \equiv \frac{y' - y'_m}{\sqrt{x^*}} \quad (4)$$

and y'_m is the y' value at which the superposed wake velocity is a minimum. The coefficients C_n assume the following values:

For $\eta < -10$,

$$C_n = 0 \quad (5)$$

For $-10 < \eta < 0$,

$$\begin{aligned} C_0 &= 0.587, & C_1 &= 0.202264, & C_2 &= 7.90697 \times 10^{-3} \\ C_3 &= -6.90281 \times 10^{-3}, & C_4 &= -1.3746 \times 10^{-3} \\ C_5 &= -1.02122 \times 10^{-4}, & C_6 &= -2.72423 \times 10^{-6} \end{aligned} \quad (6)$$

For $0 < \eta < 8$,

$$\begin{aligned} C_0 &= 0.587, & C_1 &= 0.198703, & C_2 &= 5.08547 \times 10^{-3} \\ C_3 &= -0.0206133, & C_4 &= 4.97013 \times 10^{-3} \\ C_5 &= -4.83879 \times 10^{-4}, & C_6 &= 1.73537 \times 10^{-5} \end{aligned} \quad (7)$$

For $\eta > 8$,

$$\sum_0^6 C_n \eta^n = 1 \quad (8)$$

The temperature due to the free shear layer component is found from the Crocco relation:

$$\begin{aligned} \left(\frac{T}{T_1}\right)_{\text{FSL}} &= 1 + \frac{\gamma - 1}{2} M_1^2 \left[1 - \left(\frac{u}{u_1}\right)_{\text{FSL}}^2 \right] + \left[\frac{1 - (T_2/T_1)}{1 - (u_2/u_1)} \right. \\ &\quad \left. + \frac{\gamma - 1}{2} M_1^2 \left(1 + \frac{u_2}{u_1} \right) \right] \left[\left(\frac{u}{u_1}\right)_{\text{FSL}} - 1 \right] \end{aligned} \quad (9)$$

with which the Mach number at any point is obtained:

$$M_{\text{FSL}} = \left(\frac{u}{u_1}\right)_{\text{FSL}} M_1 \left(\frac{T_1}{T}\right)_{\text{FSL}}^{1/2} \quad (10)$$

IV. Wake Component

An analytic solution for the wake of a flat plate was given in Ref. 9. A brief description of the background leading to this theory starts with the solutions found by Gold.¹⁰ Using the Oseen linearization for the momentum integral, Gold provided analytic expressions for the velocity and the temperature in the wake as functions of the boundary-layer momentum thickness at the TE of the plate. In Ref. 9 the TE velocity profiles were taken to be exponentials, the appropriate space coordinates were found again to be x' and y' as in Eq. (2), and allowance was made for $\theta_1 \neq \theta_2$. For unity Prandtl number and a constant Chapman-Rubens parameter, the nondimensional velocity and temperature in the wake were then found to be

$$\bar{u} \equiv 1 - \frac{u}{u_e} = \frac{1}{2} e^{-(y'^2/4x')} [e^{a^2} \operatorname{erfc}(a) + e^{b^2} \operatorname{erfc}(b)] \quad (11)$$

$$\bar{h} \equiv \frac{T}{T_e} - 1 = B\bar{u} + \frac{C}{2} e^{-(y'^2/4x')} [e^{c^2} \operatorname{erfc}(c) + e^{d^2} \operatorname{erfc}(d)] \quad (12)$$

where

$$P \equiv \theta_1/\theta_2 \quad (13)$$

$$a \equiv (P+1)\sqrt{x'} + \frac{y'}{2\sqrt{x'}}, \quad b \equiv \frac{P+1}{P}\sqrt{x'} - \frac{y'}{2\sqrt{x'}} \quad (14)$$

$$c \equiv 2(P+1)\sqrt{x'} + \frac{y'}{2\sqrt{x'}}, \quad d \equiv 2\frac{P+1}{P}\sqrt{x'} - \frac{y'}{2\sqrt{x'}} \quad (15)$$

$$B \equiv \frac{\gamma-1}{2} M_e^2 + \frac{T_w}{T_e} - 1, \quad C \equiv -\frac{\gamma-1}{2} M_e^2 \quad (16)$$

and where $(\cdot)_e$ signifies the constant properties external to the wake. [Equations (11) and (12) are algebraically simpler but otherwise identical to the results of Ref. 9.]

Reference 9 indicates that the preceding solutions are analytical and continuous in the desired interval $0 < x^* < \infty$, $-\infty < \tilde{y}^* < \infty$, which is in very good agreement with Goldstein's¹ $P=1$ wake solutions on the plane $y^* = \tilde{y}^* = 0$, and reduce to the linearized wake solutions³ far from the TE. This is so despite the Oseen linearization used, which in principle restricts the validity of solutions to $\bar{u}, \bar{h} \ll 1$.

As Fig. 2 shows, it is an important feature of this wake solution that for $P \neq 1$ ($\theta_1 \neq \theta_2$) the minimum of the wake velocity downstream of the TE deflects toward the side with an initially thicker boundary layer. In terms of the x', y' coordinates this deflection is called y'_m , which is the y' value zeroing the y' derivative of Eq. (11). Note that $y'_m = y'_m(x'; P) = y'_m(\bar{x}; P)$, where

$$\bar{x} \equiv \frac{x^*}{\theta_1^2 Re_1} \quad (17)$$

and that $y'_m(\bar{x}; P=1) = 0$. The deflection $y'_m(\bar{x}; P)$, shown in Fig. 3, will become significant later when the wake and FSL components are combined.

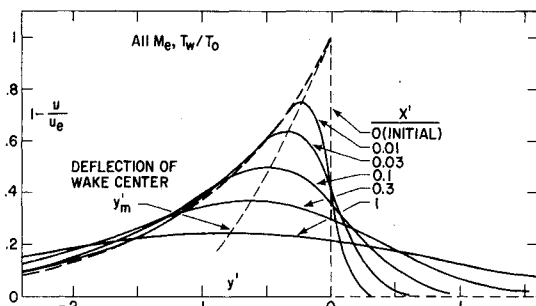


Fig. 2 Typical velocity profiles for the asymmetric ($P=0, S=1$) wake of a flat plate, from Eq. (11).

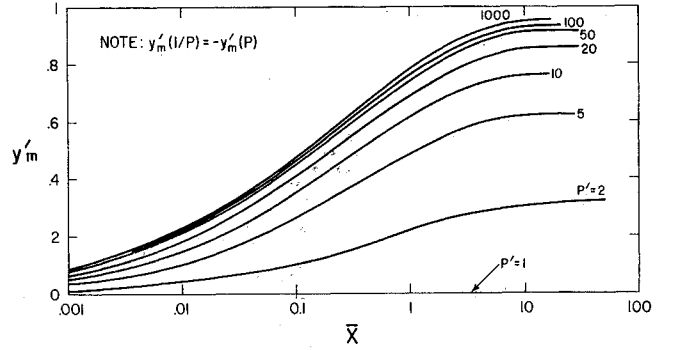


Fig. 3 The deflection y'_m of an asymmetric wake for various values of the asymmetry parameter $P = \theta_1/\theta_2$.

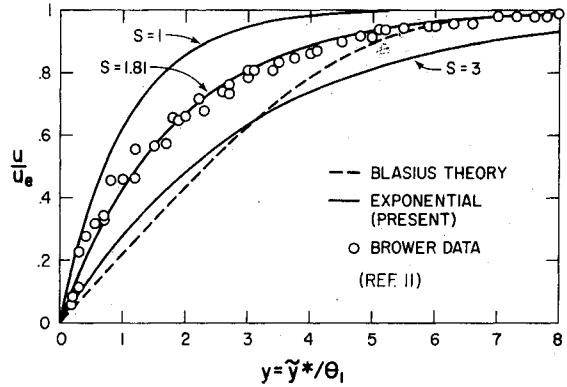


Fig. 4 Representation of a laminar boundary-layer profile by the exponential of Eq. (19).

The results of Ref. 9, as just presented, are suitable for initial velocity profiles $\bar{u}_0(\tilde{y}^* > 0) = \exp(-y)$ and $\bar{u}_0(\tilde{y}^* < 0) = \exp(Py)$ at the trailing edge, where $y \equiv \tilde{y}^*/\theta_1$, and for the corresponding temperature profiles \bar{h}_0 found from \bar{u}_0 by the Crocco relation. Figure 4 shows that this \bar{u}_0 differs considerably from the laminar (Blasius) zero-pressure-gradient (ZPG) profile. Flexibility in simulating other laminar profiles, according to this figure, can be gained by considering $\bar{u}_0(\tilde{y}^* > 0) = \exp(-y/S)$ and $\bar{u}_0(\tilde{y}^* < 0) = \exp(Py/S)$, where the "stretching factor" S is an input parameter; for example, laminar boundary-layer velocity profiles recently obtained by Brower and Demetriades¹¹ in the accelerating flow of a supersonic nozzle are fitted quite well by $S=1.8$. In the solutions (11–16), y' would then be replaced by y'/S . However, this would stretch the profiles downstream of the TE about the zero streamline $y^* = \tilde{y}^* = y' = 0$, whereas it appears more reasonable to do the stretching about the wake minimum at y'_m . Thus, we seek a new variable y'' to replace y' in Eqs. (14) and (15) and to obey the conditions $y''(x^*=0) = y'/S$, $y''(S=1) = y'$, $y''(y' = y'_m) = y'_m$, and $y''(y'_m=0) = y'/S$. The variable that satisfies these conditions is

$$y'' = \frac{y' + (S-1)y'_m}{S} \quad (18)$$

The end result for the wake of a flat plate is therefore the same equations (11–16) with y' replaced by y'' . The corresponding TE boundary-layer profiles are

$$y, y^*, \tilde{y}^*, y' > 0: \bar{u}_0 = e^{-y/S}$$

$$\bar{h}_0 = Be^{-y/S} + Ce^{-2y/S} = B\bar{u}_0 + Ce^{-2y/S} \quad (19)$$

$$y, y^*, \tilde{y}^*, y' < 0: \bar{u}_0 = e^{Py/S}$$

$$\bar{h}_0 = Be^{Py/S} + Ce^{2Py/S} = B\bar{u}_0 + Ce^{2Py/S} \quad (20)$$

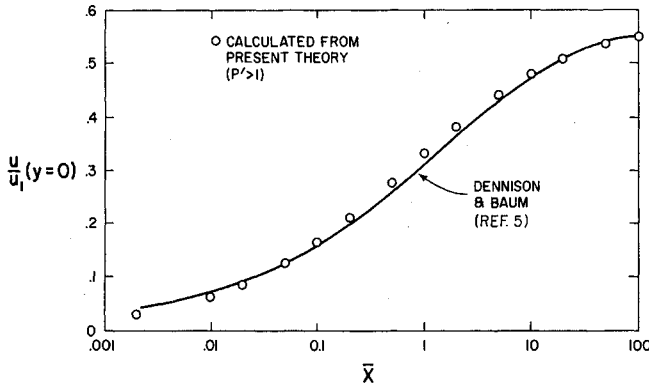


Fig. 5 Comparison of the present theory [Eq. (32), with $u_2 = 0$, $P' > 1$] with the computations of Ref. 5.

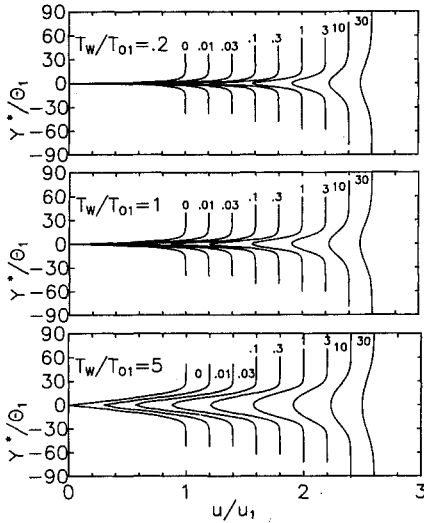


Fig. 6 Effect of the plate temperature T_w on the symmetric wake velocity profiles at low speeds [from Eq. (32), with $u_2 = u_1$, $M_1 = 0$, $\theta_1 = \theta_2$, $T_{02} = T_{01}$].

V. Combination of FSL and Wake Components

When $(\cdot)_1 \neq (\cdot)_2$, it is necessary to account for $\rho_1 \neq \rho_2$ generally; therefore, the compressible-transformed counterpart of y^* for the TE boundary layers must properly be

$$y^* > 0: \tilde{y}^* = \int_0^{y^*} \frac{\rho}{\rho_1} dy^* \quad (21)$$

$$y^* < 0: \tilde{y}^* = \int_0^{y^*} \frac{\rho}{\rho_2} dy^* \quad (22)$$

and it can be easily shown that the assumed exponential initial profiles must then be rewritten as follows for $y^* < 0$:

$$\tilde{u}_0 = e^{P'y/S} \quad (23)$$

$$\tilde{h}_0 = B\tilde{u}_0 + Ce^{2P'y/S} \quad (24)$$

where $P' = \theta_1 \rho_1 / \theta_2 \rho_2$ is the asymmetry parameter modified from Eq. (13) to account for density differences.

With these modifications the equations for the wake component are

$$\frac{u}{u_e} = 1 - \tilde{u} = 1 - \frac{1}{2} e^{-(y'^2/4x')} [e^{a'^2} \text{erfc}(a') + e^{b'^2} \text{erfc}(b')] \quad (25)$$

$$\frac{T}{T_e} = 1 + \tilde{h} = 1 + B\tilde{u} + \frac{C}{2} e^{-(y'^2/4x')} [e^{c'^2} \text{erfc}(c') + e^{d'^2} \text{erfc}(d')] \quad (26)$$

$$a' \equiv (P' + 1)\sqrt{x'} + \frac{y''}{2\sqrt{x'}}, \quad b' \equiv \frac{P' + 1}{P'} \sqrt{x'} - \frac{y''}{2\sqrt{x'}} \quad (27)$$

$$c' \equiv 2(P' + 1)\sqrt{x'} + \frac{y''}{2\sqrt{x'}}, \quad d' \equiv 2\frac{P' + 1}{P'} \sqrt{x'} - \frac{y''}{2\sqrt{x'}} \quad (28)$$

$$B \equiv \frac{\gamma - 1}{2} M_{FSL}^2 + \frac{T_w}{T_{FSL}} - 1, \quad C \equiv -\frac{\gamma - 1}{2} M_{FSL}^2 \quad (29)$$

when the initial boundary-layer profiles are as given by Eqs. (19), (23), and (24). Note that the Mach number in B and C now uses Eq. (10) to reflect the replacement of a uniform stream by that distorted by the inviscid asymmetry, and that

$$\frac{T_w}{T_{FSL}} = \frac{T_w}{T_{01}} \frac{T_1}{T_{FSL}} \quad (30)$$

with the last ratio given by Eq. (9).

The two components can now be joined by postulating that the first ratio in the identity

$$\frac{u}{u_1} = \left(\frac{u}{u_{FSL}} \right) \left(\frac{u_{FSL}}{u_1} \right) \quad (31)$$

is replaceable by the u/u_e of Eq. (25), meaning that the background flow for the wake growth is now that produced by the inviscid asymmetry; thus, combining Eqs. (3) and (25),

$$\frac{u}{u_1} = \left(\frac{u}{u_e} \right)_{\text{wake}} \left(\frac{u}{u_1} \right)_{FSL} = \left\{ 1 - \frac{1}{2} e^{-(y'^2/4x')} [e^{a'^2} \text{erfc}(a') + e^{b'^2} \text{erfc}(b')] \right\} \left[\left(1 - \frac{u_2}{u_1} \right) \sum_0^6 C_n \eta^n + \frac{u_2}{u_1} \right] \quad (32)$$

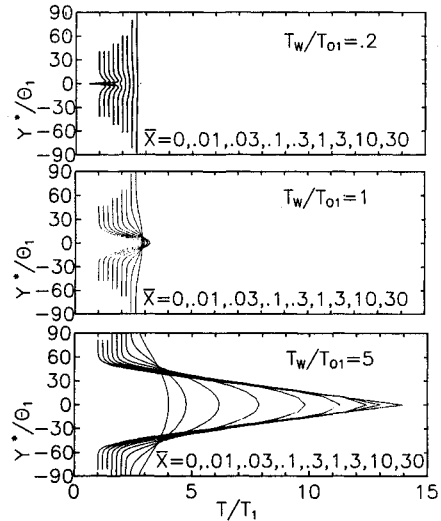


Fig. 7 Effect of plate temperature T_w on the symmetric Mach 3 wake temperature profiles [from Eq. (33), with $u_2 = u_1$, $M_1 = 3$, $\theta_1 = \theta_2$, $T_{02} = T_{01}$].

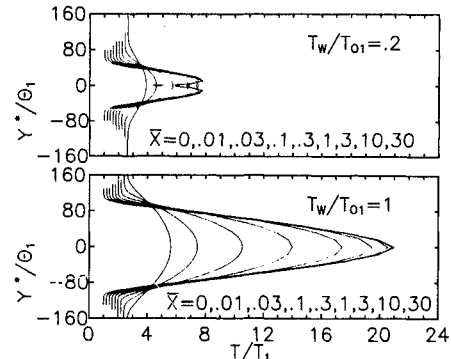


Fig. 8 Effect of plate temperature T_w on the symmetric Mach 10 wake temperature profiles [from Eq. (33) with $u_2 = u_1$, $M_1 = 10$, $\theta_1 = \theta_2$, $T_{02} = T_{01}$].

Similarly,

$$\frac{T}{T_1} = \left(\frac{T}{T_e} \right)_{\text{wake}} \left(\frac{T}{T_1} \right)_{\text{FSL}} \quad (33)$$

with the first ratio in Eq. (33) obtainable from Eq. (26) and the second from Eq. (9). A subtle point in this "composite" scheme concerns the relative lateral placement of the two components. The solutions of Sec. IV for the wake component provided as $u/u_e = u/u_e(x', y''; P')$ retain the $y'' = y'_m$ point as the minimum in the velocity profile. This minimum reasonably separates the two sides of the wake and acts as a "dividing streamline" of the two original streams. Therefore, it is necessary that what is known as the "zero streamline" in the original $u_2 = 0$ Chapman solutions (e.g., the point where $u/u_1 = 0.587$) also coincides with this dividing streamline. This explains, and is already assured by, the choice of the Chapman variable η in Eq. (4), which becomes zero at $y' = y'_m$. The quantity y'_m can be calculated analytically, as mentioned earlier, and in the present case of combined flows it is the y'' value for which the y'' derivative of Eq. (25) becomes zero; it can also be obtained from Fig. 3 if P' is put in the place of P .

VI. Comparison with Numerical Solutions

Equations (32) and (33) provide continuous closed-form solutions for the velocity and temperature over the entire range $0 < x' < \infty$, $-\infty < y' < \infty$, which reduce to the initial profiles at $x' = 0$, to familiar asymptotic solutions at $x' = \infty$ and to the given boundary conditions at $y' = \pm \infty$. The solu-

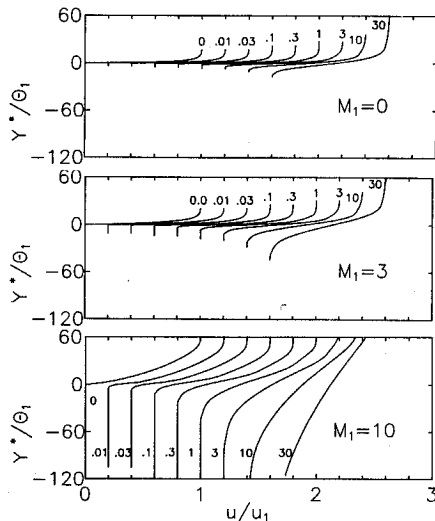


Fig. 9 Effect of edge Mach number M_1 on the velocity profiles of a shear layer adjacent to a stagnant ("base flow") region cooled to $T_w/T_{01} = T_{02}/T_{01} = 0.2$ [Eq. (32) with $u_2 = 0$, $\theta_1 > \theta_2$].

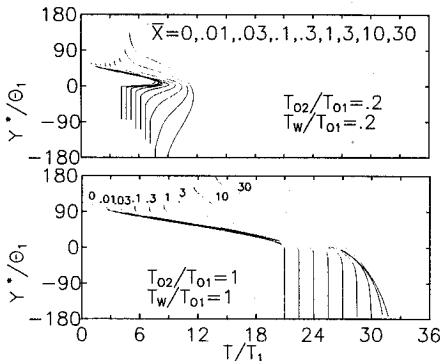


Fig. 10 Effect of wall and stagnant-region temperatures T_w and T_{02} on the temperature profiles of a hypersonic (Mach 10) "base flow" [Eq. (33), with $M_1 = 10$, $\theta_1 > \theta_2$, $u_2 = 0$].

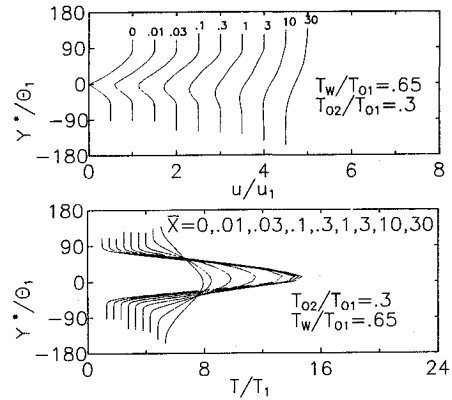


Fig. 11 Film cooling velocity and temperature profiles downstream of a partition initially separating a hypersonic flow from a cooled supersonic flow [Eqs. (32) and (33), with $M_1 = 10$, $u_2 = u_1 = 0.5$, $\theta_1/\theta_2 = 1$].

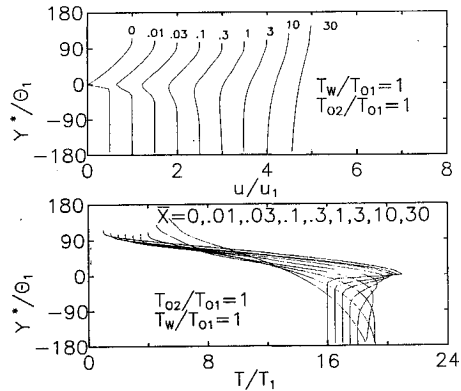


Fig. 12 Film cooling velocity and temperature profiles downstream of a partition initially separating a hypersonic flow from a supersonic flow of equal stagnation temperature [Eqs. (32) and (33), with $M_1 = 10$, $u_2/u_1 = 0.5$, $\theta_1/\theta_2 = 1$].

tions for u/u_1 and T/T_1 are both functions of the space coordinates x^*, y^* and the seven input parameters γ , M_1 , S , P' , u_2/u_1 , T_{02}/T_{01} and T_w/T_{01} . Comparison with other analyses, numerical computations, or experiments can be made easily by choosing these parameters appropriately. A comparison with the flat-plate plane-of-symmetry wake results provided by Goldstein¹ has already been made in Ref. 9. To simulate this flow, Eq. (32) is used with $P' = u_2/u_1 = 1$ and $y^* = 0$ (meaning $y = y' = y'' = 0$). As shown by Ref. 9, Goldstein's results are duplicated very closely by Eq. (32).

A comparison was also made with the computation by Dennison and Baum⁵ of a separated boundary layer flowing adjacent to a recirculation zone ($u_2 \approx 0$). The Dennison-Baum results for $y^* = \bar{y}^* = 0$ are shown by the solid line in Fig. 5, plotted vs the \bar{x} parameter of Eq. (17). The points shown on the same figure are supplied by Eq. (32) using $u_2/u_1 = y' = 0$. The points were computed for $S = 3$, although other initial profile shapes in the range $1 < S < 3$ changed the result by 3% at most, meaning that the initial profile shape (for fixed θ_1) is unimportant. [This conclusion applies strictly for the present case where the fluid with conditions $()_2$ extends to $y^* = -\infty$.] The P' parameter was taken larger than unity, to signify a greater momentum loss by the separating than the recirculating flow (the points shown change very little in the range $1 < P' < \infty$). The agreement shown in Fig. 5 is very good indeed; momentum-integral methods⁶ have shown a poorer agreement.

VII. Applications

As indicated, a variety of flowfields can be calculated with Eqs. (32) and (33) by the proper choice of the seven input parameters. Ordinary flat-plate wakes are obtained for $()_1 = ()_2$, whether symmetric or not (depending on P) and

whether or not the plate temperature differs from the total stream temperature ($T_w \neq T_{01}$). Flows of the "base" or "separated" variety are obtained for $u_2/u_1 = 0$, and "partition" flows with $(\cdot)_1 \neq (\cdot)_2$ generally can be calculated for two streams mixing downstream of a thin partition. Many such examples are illustrated in Ref. 12, a few of which are also shown here in Figs. 6–12, for the dual purpose of demonstrating the technique and illustrating various flows. In these figures the abscissa is normalized with its value in stream 1, and the ordinate is the physical distance y^* normalized with θ_1 ; negative y^*/θ_1 is on the side of stream 2. Each curve on each figure is a profile at constant \bar{x} [Eq. (17)], with the profile at $\bar{x} = 0$ (the initial boundary layers at the TE) at the extreme left of each figure. The origins for the subsequent profiles, at $\bar{x} = 0.01, 0.03, 0.1$, etc., are each displaced to the right by fixed steps for clarity.

All results shown were calculated from Eqs. (32) and (33) and, for brevity, $\gamma = 1.4$ and $S = 3$ are used throughout. Symmetric wake flows, plotted in Figs. 6–8, are obtained for $u_1 = u_2$, $P = P' = 1$, and $T_{02} = T_{01}$. In these figures the velocity and temperature profiles are shown for low-speed, supersonic, and hypersonic wakes with $M_1 = 0, 3$, and 10 , respectively. The notation $T_w/T_{01} = 0.2, 1$, and 5 indicate a cooled, adiabatic, and heated wake, respectively. For example, at Mach 10 the maximum temperature of the flow at $x^* = 30\theta_1^2 Re_1'$ is about $2.3T_1$.

The "base flow" nomenclature employed in Figs. 9 and 10 indicates the separated boundary-layer growth adjacent to a stagnant region extending infinitely toward negative y^* . This type of flow is given by Eqs. (32) and (33) when $u_2 = 0$, and, although not identical, it is related to the flow formed at the base of a bluff object and bounded by separated boundary layers. Figure 9 shows the effect of increasing M_1 on the velocity distribution beyond separation, when the surface and the base region are cooled ($T_w = T_{02} = 0.2T_{01}$); in Fig. 10 the effect is shown on the temperature profiles of cooling from $T_w = T_{02} = T_{01}$ to $T_w = T_{02} = 0.2T_{01}$ for a hypersonic condition (Mach 10). In both cases θ_1 is taken to be much larger than θ_2 , to reflect the extensive friction history of the boundary layer before separation. (As noted, these results are independent of P' for $P' > 1$.)

Finally, Figs. 11 and 12 show results for a hypersonic stream at $M_1 = 10$ separated from a "film-cooling" jet of half the speed, by a thin partition. In this instance Eqs. (32) and (33) have been used with $u_2/u_1 = 0.5$, $M_1 = 10$, $P = 1$, and $T_w = (T_{01} + T_{02})/2$, the latter typical of a very thin solid partition separating streams of unequal temperatures. For the purpose of illustrating the effect of the coolant jet temperature, Figs. 11 and 12 involve $T_{02} = 0.3T_{01}$ and $T_{02} = T_{01}$, respectively; the corresponding jet Mach numbers M_2 are 4.38 and 1.25. Note that a cooled jet (Fig. 11) prolongs the velocity minimum to large \bar{x} distances, often amounting to several thousand momentum thicknesses θ_1 .

It must be noted that the method of combining the two flow components as in Eqs. (32) and (33) is not an addition of two independent solutions of a linear equation; linearization enters the problem only through the Oseen approximation involved in the wake component formulas (11) and (12). This approximation would normally produce invalid results near the partition trailing edge; however, in the present instance the requirement that the wake solution reduces to the trailing-edge profiles at $x^* = 0$ enables Eqs. (11) and (12) to represent the entire wake flow in $0 < x^* < \infty$ very closely.⁹ The composite solutions (32) and (33) similarly depend on the linearized wake component, but once again in such a manner that the initial and asymptotic conditions are satisfied and that, as Figs. 6–12 show, reasonable results are produced at intermediate regions.

Acknowledgments

Support for this work was provided by the Los Alamos National Laboratory and by the Rocketdyne Division of Rockwell International Corporation. The author acknowledges with gratitude the assistance of Fred L. Yapuncich with the computation and graphics of the numerical examples.

References

- ¹Goldstein, S., "Concerning Some Solutions of the Boundary Layer Equations in Hydrodynamics," *Proceedings of the Cambridge Philosophical Society*, Vol. 26, 1930, pp. 1–30.
- ²Goldstein, S., "On the Two-Dimensional Steady Flow of a Viscous Fluid Behind a Solid Body — I, II," *Proceedings of the Royal Society of London, Series A*, Vol. 142, 1933, pp. 545–573.
- ³Tollmien, W., "Boundary Layers," *Handbook of Experimental Physics*, Vol. 4, *Hydro- and Aerodynamics*, P. 1, Akademie Verlag, Leipzig, GDR, 1931, p. 267.
- ⁴Chapman, D. R., "Laminar Mixing of a Compressible Fluid," NACA TR-958, Jan. 1950.
- ⁵Dennison, M. R., and Baum, E., "Compressible Free Shear Layer With Finite Initial Thickness," *AIAA Journal*, Vol. 1, Feb. 1963, pp. 342–349.
- ⁶Kubota, T., and Dewey, C. F., Jr., "Momentum Integral Methods for the Laminar Free Shear Layer," *AIAA Journal*, Vol. 2, April 1964, pp. 625–629.
- ⁷Ragab, S. A., "Instabilities in the Wake/Mixing Layer Region of a Splitter Plate Separating Two Supersonic Streams," AIAA Paper 88-3677, 1988.
- ⁸Berger, S. A., *Laminar Wakes*, American Elsevier, New York, 1971, Chap. 2.
- ⁹Demetriades, A., "The Two-Dimensional Laminar Wake with Initial Asymmetry," *AIAA Journal*, Vol. 21, Sept. 1983, pp. 1347–1349.
- ¹⁰Gold, H., "Laminar Wake with Arbitrary Initial Profiles," *AIAA Journal*, Vol. 2, May 1964, pp. 948–949.
- ¹¹Brower, T., and Demetriades, A., "Experiments on the Free Shear Layer Between Two Supersonic Streams," AIAA Paper 90-0710, Jan. 1990.
- ¹²Demetriades, A., "Partition Flow Theory: A Novel Approach to the Mixing of Parallel Laminar Steady Flows," MSU SWT TR-89-03, Montana State University, Bozeman, MT, Sept. 1989.